

1970

Bearing capacity of concrete blocks, December 1970. (71-17)

W. F. Chen

S. Covarrubias

Follow this and additional works at: <http://preserve.lehigh.edu/engr-civil-environmental-fritz-lab-reports>

Recommended Citation

Chen, W. F. and Covarrubias, S., "Bearing capacity of concrete blocks, December 1970. (71-17)" (1970). *Fritz Laboratory Reports*. Paper 2024.
<http://preserve.lehigh.edu/engr-civil-environmental-fritz-lab-reports/2024>

This Technical Report is brought to you for free and open access by the Civil and Environmental Engineering at Lehigh Preserve. It has been accepted for inclusion in Fritz Laboratory Reports by an authorized administrator of Lehigh Preserve. For more information, please contact preserve@lehigh.edu.

BEARING CAPACITY OF CONCRETE BLOCKS

by

W. F. Chen¹

and

S. Covarrubias²

ABSTRACT

Theoretical and experimental results are presented for the bearing capacity of concrete blocks with an axially or eccentrically located cable duct and axially or eccentrically loaded by two rigid punches. The solutions have been obtained using the concept and the theory developed recently by Chen and Drucker. The agreement between the theory and experimental results is satisfactory. These solutions should provide a better understanding of the bearing strength of the anchorage zones of post-tensioned concrete members.

¹ Assistant Professor, Department of Civil Engineering, Lehigh University, Bethlehem, Pennsylvania.

² Instructor, University of Mexico, Mexico. Formerly, Research Assistant, Fritz Engineering Laboratory, Department of Civil Engineering, Lehigh University, Bethlehem, Pennsylvania.

1. INTRODUCTION

The problem of the end bearing of a post-tensioned concrete beam may be idealized and simplified to the problem of a circular cylindrical concrete block or a square prismatic concrete block with a longitudinal cable duct loaded by two circular or two square punches applied on the cable duct at both ends (Fig. 1). A complete elastic solution to the problem under the conditions of axial symmetry has been obtained by Sundara Raja Iyengar and Yogananda [1]. The three-dimensional punch problem (Fig. 1) is complicated and probably not possible for an elastic-plastic analysis, since such an analysis requires the basic knowledge of the stress-strain relations for concrete in the elastic as well as the inelastic range. No such general relations have been determined as yet for inelastic concrete. However, as in previous work [2] on the bearing capacity of concrete blocks, the limit theorems [3] of the generalized theory of perfect plasticity can be used to determine upper and lower bounds for the maximum bearing capacity of the problem.

In the following work, only the upper bound theorem of limit analysis is employed to obtain the bearing pressure which can be applied by circular and square punches. The first problem to be considered under this approach is the incipient collapse of a circular cylinder or a square block with a co-axial cable duct compressed by two forces applied centrally through two circular or square punches (Fig. 1a). The second is to extend this result to obtain the solution of a block with an eccentrically located cable duct and eccentrically loaded by two rigid punches (Fig. 1b).

Since the lower bound theorem of limit analysis is not considered in the present analysis, the solutions so obtained can at best give only upper bounds to the problem. However, the fact that the upper bound solutions obtained in Ref. 2 is found to be very close to the correct value, suggests that the same is also true for the more general case of the bearing capacity problem described in the present paper.

This paper contains a theoretical and experimental analysis of the generalized bearing capacity problem, as shown in Fig. 1. The theoretical part of the analysis includes upper bound calculations of the bearing pressure for short as well as long concrete blocks. Experiments were performed to determine the bearing capacity of the concrete blocks with various punch eccentricity ratios and to compare their results with the theoretical upper bound values. Since calculations of the upper bound solutions are sometimes laborious, simple approximate evaluations of the general bearing capacity problem for practical purposes are proposed.

2. UPPER BOUND THEOREM OF LIMIT ANALYSIS

The upper bound theorem of limit analysis [3] states that a concrete block will collapse if, for any assumed failure mechanism, the rate of work done by the applied loads exceeds the internal rate of dissipation. Equating external and internal energies for any such mechanism thus gives an upper bound on the collapse load.

As stated in the upper bound theorem, it is necessary to compare the rate of internal dissipation of energy with the rate of

work of external forces. The dissipation of energy, D_A , per unit area due to a plastic shearing is, therefore, of primary importance. The dissipation function, D_A , can be derived in a straightforward manner on the not-so-justifiable assumption of perfect plasticity. Herein, as in Ref. 2, the concrete may be idealized as perfectly plastic with a Mohr-Coulomb failure surface as the yield surface in compression and a small but non-zero tension cutoff (Fig. 2). No effort is made here to restate the fundamental arguments necessary in order to justify the validity of the theory of Ref. 2. Already available are results from a research program for the bearing capacity of some concrete blocks [4,5,6,7,8]. In Fig. 2, f'_c and f'_t denote the simple compression and simple tensile strength, respectively, C is cohesion and φ is the angle of internal friction of the concrete. The vector δw representing slip velocity with tangential slip and normal separation velocity components δu and δv , across the failure surface, is normal to the yield curve [9]. It can be shown that the dissipation function has the form [2]

$$D_A = \delta w \left(f'_c \frac{1 - \sin\theta}{2} + f'_t \frac{\sin\theta - \sin\varphi}{1 - \sin\varphi} \right) \quad (1)$$

in which $\tan\theta = \frac{\delta v}{\delta u} \geq \tan\varphi \quad (2)$

For the particular cases of simple tensile separation and simple sliding for which $\theta = \pi/2$ and $\theta = \varphi$, respectively, Eq.(1) takes the simple forms

$$D_A = f'_t \delta v \quad \text{for } \theta = \frac{\pi}{2} \quad (3)$$

and

$$D_A = f'_c \frac{1 - \sin\varphi}{2} \delta w \quad \text{for } \theta = \varphi \quad (4)$$

3. CONCRETE BLOCKS WITH A CONCENTRIC CABLE DUCT

3.1 Short Circular and Square Blocks (Fig. 3)

Figure 3 shows a failure mechanism consisting of simple tension cracks and truncated cone or truncated pyramid rupture surfaces directly beneath the punches. The two truncated cones or pyramids of angle 2α move toward each other as rigid bodies, and displace the surrounding material horizontally sideways. The relative velocity vector δw at every point on the truncated cone or pyramid surfaces is inclined at an angle θ to the surfaces. The compatible velocity relations are also shown in Fig. 3 from which the rate of internal dissipation of energy on the surfaces of discontinuity can be calculated easily. Since the sliding surfaces of the truncated cones or pyramid involve shearing and separation, the rate of dissipation of energy is found by multiplying the area of each truncated cone or pyramid surface by the dissipation function, D_A , as given by Eq.(1). To this internal rate of dissipation has to be added the rate of dissipation obtained as the product of the area of the discontinuity surfaces for simple tensile cracks multiplied by f'_c times the separation velocity δv (Eq.3). It is found, by equating the rate at which work is done by the forces on the punches to the rate of the total internal dissipation of energy, that the value of the upper bound on the average bearing pressure over the net bearing area is

$$q^u = \frac{\frac{1 - \sin\theta}{2} f'_c + \frac{\sin\theta - \sin\varphi}{1 - \sin\varphi} f'_t}{\sin\alpha \cos(\alpha + \theta)} \quad (5)$$

$$+ \frac{\tan(\alpha + \theta) \left[\frac{h}{a} \left(\frac{b}{a} - \frac{c}{a} \right) - \left(1 - \frac{c}{a} \right)^2 \cot\alpha \right] f'_t}{1 - \left(\frac{c}{a} \right)^2}$$

The upper bound has a minimum value when $\theta = \varphi$ and α satisfies the condition

$$\cot\alpha = \tan\varphi + \sec\varphi \left\{ 1 + \frac{\frac{h}{a} \left(\frac{b}{a} - \frac{c}{a} \right) \cos\varphi}{\left[1 - \left(\frac{c}{a} \right)^2 \right] \frac{1 - \sin\varphi}{2} \frac{f'_c}{f'_t} - \left(1 - \frac{c}{a} \right)^2 \sin\varphi} \right\}^{1/2} \quad (6)$$

valid for $(1 - \frac{c}{a}) \cot\alpha \leq \frac{h}{2a}$ (7)

and Eq.(5) is reduced to

$$q^u = \frac{\left[\frac{h}{a} \left(\frac{b}{a} - \frac{c}{a} \right) \tan(2\alpha + \varphi) - \left(1 - \frac{c}{a} \right)^2 \right] f'_t}{1 - \left(\frac{c}{a} \right)^2} \quad (8)$$

For the special case for which $c/a = 0$, Eqs.(5) to (8) reduce to the equations obtained previously by Chen and Drucker [2].

The value of q^u/f'_c is plotted against $h/2a$ in Fig. 4 for a punch for which $b/a = 4$ and $c/a = 0$. Experimental results are denoted by small circles in the figure. The theoretical curve computed for $\varphi = 20^\circ$ and $f'_c = 12 f'_t$ is found to be in good agreement with the results of tests. Details of the tests will be discussed later.

3.2 Long Circular and Square Blocks (Fig. 5)

Mechanism 1 for a short block may be modified to Mechanism 2 for a long block as shown in Fig. 5. Instead of simple tensile cracks along the total height of the block, eight planes of sliding all inclined at an angle of β to the vertical are assumed. The two punches move towards each other with a relative velocity, $2\Delta_D$, and are accommodated by the sideway movements, Δ , of the eight surrounding rigid blocks, inclined at an angle of γ to the horizontal. These planes of sliding involve shearing and separation so that Eq.(1) may be used to compute the rate of dissipation of energy per unit area. The total dissipation of energy in the block can then be found by adding to this rate the rates of dissipation at other discontinuity surfaces, i.e., those due to simple tensile cracks plus truncated cone or pyramid rupture surfaces. Equating the rate at which work is done by the force on the punches to the total rate of energy dissipation in the block, it is found that an upper bound on the average bearing capacity of the punch loading is

$$\begin{aligned}
 q^u = & \frac{(1 - \frac{c}{a})^2}{1 - (\frac{c}{a})^2} \frac{(1 - \sin\varphi) \cos\gamma}{\sin\alpha \cos(\alpha + \gamma + \varphi)} \frac{f'_c}{2} \\
 & + \frac{(\frac{b}{a} - \frac{c}{a})^2}{1 - (\frac{c}{a})^2} \frac{\sin(\alpha + \varphi)}{\sin\beta \cos(\alpha + \gamma + \varphi)} \left\{ f'_c \frac{1 - \cos(\beta - \gamma)}{2} \right. \\
 & \left. + f'_t \frac{\cos(\beta - \gamma) - \sin\varphi}{1 - \sin\varphi} \right\} + \frac{\cos\gamma \sin(\alpha + \varphi) f'_t f_1(\alpha, \beta)}{\left[1 - (\frac{c}{a})^2 \right] \cos(\alpha + \gamma + \varphi)}
 \end{aligned} \quad (9)$$

where

$$f_1(\alpha, \beta) = \left(\frac{b}{a} - \frac{c}{a}\right)^2 \cot\beta + \left(2\frac{b}{a} - \frac{c}{a} - 1\right) \left(1 - \frac{c}{a}\right) \cot\alpha \quad (10)$$

This is an upper bound solution for a square punch on a square block or a circular punch on a circular cylinder. For the special case of no cable duct, $c/a = 0$ and Eq.(9) reduces to the equation obtained previously by Chen and Drucker [2]. The upper bound solution has a minimum value when α , β , and γ satisfy the conditions

$$\frac{\partial q^u}{\partial \alpha} = 0, \quad \frac{\partial q^u}{\partial \beta} = 0, \quad \text{and} \quad \frac{\partial q^u}{\partial \gamma} = 0 \quad (11)$$

Solving these equations and substituting the values of α , β , and γ thus obtained in Eq.(9), yields a least upper bound solution for the bearing capacity problem. The results of these computations are presented in Table 1 for $\varphi = 20^\circ$ and $f'_c/f'_t = 10$ and 14, respectively. The critical values of β and γ are seen to be insensitive to the dimension ratios b/a and c/a but depend mainly on the concrete strength ratio f'_c/f'_t .

The upper bounds, given by Mechanism 1 and Mechanism 2, are plotted in Fig. 6 for values of $f'_c = 10 f'_t$, $b/a = 4$, $h/2a = 10$, and $\varphi = 20^\circ$. (Note: \bar{q} = load/total punch area). It can be seen that the concrete bearing strength is relatively insensitive to c/a ratios of the cable duct when these are very small, but the strength is considerably reduced when the c/a ratios are large. When $h/2a \geq 12$, Mechanism 2 almost always governs. The concrete blocks with $h/2a \geq 12$ can therefore be considered as long blocks.

4. CONCRETE BLOCKS WITH AN ECCENTRIC CABLE DUCT -
SMALL ECCENTRICITY

4.1 Short Circular and Square Blocks (Fig. 7)

Mechanism 1 in Fig. 3 can be modified to provide an upper bound for the collapse pressure for the case of a block with an eccentrically located cable duct and eccentrically loaded by two rigid punches. Only the plan view of the modified mechanisms is shown in Fig. 7. For a circular block, it is convenient to approximate the circular punch by a regular polygon of $n = 8, 16, 32, \dots$. Mechanism 3, shown in Fig. 7, is for $n = 8$.

Following the same procedure described for Mechanism 1, the bearing capacity for a circular block is found to be

$$q^u = \frac{n}{\pi} \frac{(1 - \sin\varphi) \tan \frac{\pi}{n} \frac{f'_c}{2}}{\sin\alpha \cos(\alpha + \varphi)} + \frac{4 \tan(\alpha + \varphi) \tan \frac{\pi}{n}}{\pi \left[1 - \left(\frac{c}{a}\right)^2 \right]}$$

$$\left\{ \frac{b}{a} \frac{h}{a} \cos \frac{\pi}{n} \sum_{i=1}^{n/4} \left[1 - \left(\frac{e}{b}\right)^2 \sin^2 \frac{(2i-1)\pi}{n} \right]^{1/2} - \frac{c}{a} \frac{h}{a} - \frac{n}{4} \left(1 - \frac{c}{a} \right)^2 \cot\alpha \right\} f'_t \quad (12)$$

The value of q^u is minimum when

$$\cot\alpha = \tan\varphi + \sec\varphi \left\{ 1 + \frac{\frac{h}{a} \frac{b}{a} \cos\varphi \cos \frac{\pi}{n} \sum_{i=1}^{n/4} \left[1 - \left(\frac{e}{b}\right)^2 \sin^2 \frac{(2i-1)\pi}{n} \right]^{1/2} - \frac{c}{a} \frac{h}{a} \cos\varphi}{\frac{n}{8} \frac{f'_c}{f'_t} (1 - \sin\varphi) \left[1 - \left(\frac{c}{a}\right)^2 \right] - \frac{n}{4} \left(1 - \frac{c}{a} \right)^2 \sin\varphi} \right\}^{1/2} \quad (13)$$

and Eq. (12) reduces to

$$q^u = \frac{\tan \frac{\pi}{n} \tan(2\alpha + \varphi)}{1 - \left(\frac{c}{a}\right)^2} \left\{ \frac{b}{a} \frac{h}{a} \cos \frac{\pi}{n} \sum_{i=1}^{n/4} \left[1 - \left(\frac{e}{b}\right)^2 \sin^2 \frac{(2i-1)\pi}{n} \right]^{1/2} \right. \\ \left. - \frac{c}{a} \frac{h}{a} - \frac{n}{4} \left(1 - \frac{c}{a}\right)^2 \cot(2\alpha + \varphi) \right\} f'_t \quad (14)$$

$$\text{valid for} \quad \cot \alpha \leq \frac{h}{2a} \quad (15)$$

By comparing the values of the average bearing pressure computed from Eq. (14) for $n = 8$ and $n = 64$, respectively, it is found that the bearing pressure is not sensitive to the value of n , and thus $n = 8$ may be considered as a suitable value in Eq. (14) for all practical purposes.

Similarly, the bearing capacity for a square punch on a square block is found to be (Mechanism 4, Fig. 7)

$$q^u = \frac{1 - \sin \varphi}{\sin \alpha \cos(\alpha + \varphi)} \frac{f'_c}{2} + \frac{\frac{h}{a} \left[2 \left(\frac{b}{a} - \frac{c}{a}\right) - \frac{e}{b} \frac{b}{a} \right] \tan(\alpha + \varphi) \frac{f'_t}{2}}{1 - \left(\frac{c}{a}\right)^2} \\ - \frac{\left(1 - \frac{c}{a}\right)^2}{1 - \left(\frac{c}{a}\right)^2} \cot \alpha \tan(\alpha + \varphi) f'_t \quad (16)$$

The value of q^u is minimum when

$$\cot \alpha = \tan \varphi + \sec \varphi \left\{ 1 + \frac{\frac{1}{2} \frac{h}{a} \left[2 \left(\frac{b}{a} - \frac{c}{a}\right) - \frac{e}{b} \frac{b}{a} \right] \cos \varphi}{\left[1 - \left(\frac{c}{a}\right)^2 \right] \frac{1 - \sin \varphi}{2} \frac{f'_c}{f'_t} - \left(1 - \frac{c}{a}\right)^2 \sin \varphi} \right\}^{1/2} \quad (17)$$

and Eq.(16) reduces to

$$q^u = \frac{f_t}{2} \frac{h}{a} \frac{\left[2 \left(\frac{b}{a} - \frac{c}{a} \right) - \frac{e}{b} \frac{b}{a} \right] \tan(2\alpha + \varphi) - \left(1 - \frac{c}{a} \right)^2}{1 - \left(\frac{c}{b} \right)^2} \quad (18)$$

valid for $(1 - \frac{c}{a}) \cot\alpha \leq \frac{h}{2a}$ (19)

4.2 Long Square Blocks (Fig. 8)

A direct extension of the eccentrically loaded situation of Mechanism 2 (Fig. 5) for a square block is shown in Fig. 8 (vertical section only). Mechanism 2' is evident in Fig. 8. It is found that the equation for computing the bearing capacity pressure remains identical in its form as in the previous solution (Eq.9), but the function $f_1(\alpha, \beta)$ defined by Eq.(10) must be substituted by

$$f_2(\alpha, \beta) = \left[\frac{b}{a} \left(2 - \frac{e}{b} \right) - \frac{c}{a} - 1 \right] \left(1 - \frac{c}{a} \right) \cot\alpha$$

$$+ \frac{1}{2} \left[\left(\frac{b}{a} - \frac{c}{a} \right)^2 + \frac{b}{a} \left(1 - \frac{e}{b} \right) - \frac{c}{a} \right] \cot\beta \quad (20)$$

5. CONCRETE BLOCKS WITH AN ECCENTRIC CABLE DUCT - LARGE ECCENTRICITY

Mechanisms 5 through 8 are shown in Figs. 9 and 10 and need no detailed explanation. The procedure in obtaining the bearing capacity equations for various mechanisms is identical to the previous cases, and, hence, only the final results are recorded here for the sake of brevity.

5.1 Short Circular Blocks (Mechanism 5, Fig. 9)

$$q^u = \frac{f'_c}{\pi} \frac{(1 - \sin\varphi) K}{\left[1 - \left(\frac{c}{a}\right)^2\right] \sin\alpha \cos(\alpha + \varphi)}$$

$$+ \frac{f'_t}{\pi} \frac{\left\{ \frac{b}{a} + \frac{b}{a} \left[2 - \left(\frac{e}{b}\right)^2\right]^{1/2} - 3 \frac{c}{a} \right\} \frac{h}{a} - 2 \left[\left(1 - \frac{c}{a}\right)^2 + \frac{b}{a} \left(1 - \frac{e}{b}\right) - \frac{c}{a} \right] \cot\alpha}{\left[1 - \left(\frac{c}{a}\right)^2\right] \cot(\alpha + \varphi)}$$

(21)

in which

$$K = 1 - 2 \left(\frac{c}{a}\right)^2 + \left[\left(\frac{b}{a}\right)^2 - 1 \right]^{-1/2} - \frac{e}{b} \frac{b}{a}$$

$$+ \frac{1}{2} \left(\frac{b}{a}\right)^2 \left\{ \frac{\pi}{2} - \sin^{-1} \left[1 - \left(\frac{a}{b}\right)^2 \right]^{1/2} - \left[1 - \left(\frac{a}{b}\right)^2 \right]^{1/2} \cos \sin^{-1} \left[1 - \left(\frac{a}{b}\right)^2 \right]^{1/2} \right\}$$

(22)

The value of q^u is minimum when

$$\cot\alpha = \tan\varphi + \sec\varphi \left\{ 1 + \frac{\frac{h}{a} \frac{b}{a} + \frac{h}{a} \frac{b}{a} \left[2 - \left(\frac{e}{b}\right)^2\right]^{1/2} - 3 \frac{h}{a} \frac{c}{a}}{K (1 - \sin\varphi) \sec\varphi \frac{f'_c}{f'_t} - 2 \left[\left(1 - \frac{c}{a}\right)^2 + \frac{b}{a} \left(1 - \frac{e}{b}\right) - \frac{c}{a} \right] \tan\varphi} \right\}^{1/2}$$

(23)

and Eq. (21) can be reduced to

$$q^u = \frac{f'_t}{\pi} \frac{\left\{ \frac{b}{a} + \frac{b}{a} \left[2 - \left(\frac{e}{b} \right)^2 \right]^{1/2} - 3 \frac{c}{a} \right\} \frac{h}{a} \tan(2\alpha + \varphi) - \left[\left(1 - \frac{c}{a} \right)^2 + \frac{b}{a} \left(1 - \frac{e}{b} \right) - \frac{c}{a} \right]}{1 - \left(\frac{c}{a} \right)^2} \quad (24)$$

valid for $\cot\alpha \leq \frac{h}{2a}$ (Eq.14).

5.2 Short Square Blocks (Mechanism 6, Fig. 9)

$$q^u = \frac{f'_c}{4} \frac{\left[\frac{b}{a} \left(1 - \frac{e}{b} \right) - 2 \left(\frac{c}{a} \right)^2 + 1 \right] (1 - \sin\varphi)}{\left[1 - \left(\frac{c}{a} \right)^2 \right] \sin\alpha \cos(\alpha + \varphi)} + \frac{f'_t}{2} \frac{\frac{3}{2} \frac{h}{a} \left(\frac{b}{a} - \frac{c}{a} \right) - \frac{1}{2} \frac{h}{a} \frac{b}{a} \frac{e}{b} - \left[\left(1 - \frac{c}{a} \right)^2 + \frac{b}{a} \left(1 - \frac{e}{b} \right) - \frac{c}{a} \right] \cot\alpha}{\left[1 - \left(\frac{c}{a} \right)^2 \right] \cot(\alpha + \varphi)} \quad (25)$$

The value of q^u is minimum when

$$\cot\alpha = \tan\varphi + \sec\varphi \left\{ 1 + \frac{\frac{h}{2a} \left[3 \left(\frac{b}{a} - \frac{c}{a} \right) - \frac{e}{b} \frac{b}{a} \right] \cos\varphi}{\left[\frac{b}{a} \left(1 - \frac{e}{b} \right) - 2 \left(\frac{c}{a} \right)^2 + 1 \right] \frac{(1 - \sin\varphi)}{2} \frac{f'_c}{f'_t} - \left[\left(1 - \frac{c}{a} \right)^2 + \frac{b}{a} \left(1 - \frac{e}{b} \right) - \frac{c}{a} \right] \sin\varphi} \right\}^{1/3} \quad (26)$$

and Eq.(26) can be reduced to

$$q^u = \frac{f'_t}{2} \frac{\left[3 \left(\frac{b}{a} - \frac{c}{a} \right) - \frac{e}{b} \frac{b}{a} \right] \frac{h}{2a} \tan(2\alpha + \varphi) - \left[\left(1 - \frac{c}{a} \right)^2 + \frac{b}{a} \left(1 - \frac{e}{b} \right) - \frac{c}{a} \right]}{1 - \left(\frac{c}{a} \right)^2} \quad (27)$$

valid for $\cot\alpha \leq \frac{h}{2a}$ (Eq.15).

5.3 Long Circular Blocks (Mechanism 7, Fig. 10)

The velocity vector, δw , of the volume A-B-D-C-E is inclined at an angle φ to the two sliding surfaces A-B-E and A-C-E, respectively (or at an angle Ψ to the diagonal line A-E). The line A-E makes an angle β to the horizontal.

$$\begin{aligned}
 q^u = & \frac{f'c}{2\pi} \frac{(1 - \sin\varphi) [1 + \csc^2\delta \tan^2\beta]^{1/2}}{\sin(\beta - \Psi) \sin\beta} \left\{ \cot\delta \right. \\
 & + \left(\frac{b}{a}\right)^2 \left[\delta + \sin^{-1} \left(\frac{a}{b} - \frac{e}{b} \sin\delta \right) \right] \\
 & + \left(1 - \frac{e}{b} \frac{b}{a} \sin\delta\right) \left[\left(\frac{b}{a}\right)^2 - \left(1 - \frac{e}{b} \frac{b}{a} \sin\delta\right)^2 \right]^{1/2} \\
 & \left. - \frac{e}{b} \frac{b}{a} \left(2 - \frac{e}{b} \frac{b}{a} \sin\delta\right) \cos\delta \right\}
 \end{aligned} \tag{28}$$

in which the angle Ψ must satisfy the geometric condition

$$\sin\varphi = \left[\tan\beta - \tan(\beta - \Psi) \right] \cos(\beta - \Psi) \left[\sin \tan^{-1} (\sin\delta \cot\beta) \right] \tag{29}$$

The upper bound solution has a minimum value when β and δ satisfy the conditions

$$\frac{\partial q^u}{\partial \beta} = 0 \quad \text{and} \quad \frac{\partial q^u}{\partial \delta} = 0 \tag{30}$$

Solving these equations and substituting the values of β and δ thus obtained into Eq. (28), yields a least upper bound solution. Thus,

for a punch for which $b/a = 4$ and $\varphi = 20^\circ$, for example, the upper bound has the minimum value $3.31 f'_c$ or $2.58 f'_c$ when β , δ , and ψ are approximately 60° , 60° , and 22.4° for $e/b = 2/3$ or 60° , 55° , and 23° for $e/b = 3/4$, respectively.

5.4 Long Square Blocks (Mechanism 8, Fig. 10)

$$q^u = \frac{f'_c}{8} \frac{(1 + \frac{b}{a}) \left[1 + \frac{b}{a} (1 - \frac{e}{b}) \right] (1 - \sin\varphi) (2 + \tan^2\beta)}{(1 + \cos^2\beta - 2\sin^2\varphi)^{1/2} \tan\beta - 2\sin\varphi} \quad (31)$$

in which ψ must satisfy the geometric condition

$$\sin\psi = \frac{\sqrt{2} \sin\varphi}{\cos\beta \left[2 + \tan^2\beta \right]^{1/2}} \quad (32)$$

The upper bound has a minimum value when it satisfies the condition $\partial q^u / \partial \beta = 0$. Thus, for example, for a punch for which $b/a = 4$ and $\varphi = 20^\circ$, the upper bound has the minimum value near the point $\beta = 60^\circ$ and $\psi = 25.6^\circ$. The value is $4.52 f'_c$ for $e/b = 2/3$ and $3.85 f'_c$ for $e/b = 3/4$.

Figure 11 shows the values of the q^u/f'_c ratio for square blocks with various eccentricity ratios e/b . The results of calculations made with various mechanisms are calculated for concrete with $f'_c = 10 f'_t$ and $\varphi = 20^\circ$ and for a punch with $b/a = 4$ and $c/a = 0$.

Tresca's yield criterion for metals may be considered as a special concrete for which $\varphi = 0^\circ$. Equations (28) through (32) then reduce to the upper bound solutions obtained previously [10] for the plastic indentation of metal blocks by flat punches.

6. COMPARISON WITH TEST RESULTS

6.1 Present Test Results

The concrete used for the tests consisted of 1 cement to 1.6 sand to 1.5 crushed aggregate (nominal diameter, 1/2-inch) to 0.4 water by weight. In order to increase the tensile strength and ductility of concrete, 2 percent in volume of 1-inch long wire was added into and mixed randomly with the concrete, following the conclusions reported in Ref. 7.

Specimen diameter and punch diameter were constant at 6 in. and 1.5 in., respectively. The height of the cylinder was varied from 4 in. to 10 in., and three different eccentricity ratios, $e/b = 0, 1/3,$ and $2/3,$ were used in tests. The specimens were tested at an age of 21 days in a Baldwin Hydraulic Testing Machine. All specimens were moisture-cured at 75°F for two weeks to minimize drying out effects.

A spherical seat was placed on top of the top short steel cylinder (punch) and the bottom short steel cylinder was supported directly on the steel bed of the testing machine (Fig. 1). Loads were applied to the specimens continuously until failure occurred at a rate about 1 kip every 10 sec. The control tests were carried out on standard concrete cylinders. The average direct tensile strength f'_t was estimated to be 0.8 times the indirect tensile test (splitting).

Test results and upper bound solutions are summarized in columns 7 and 8 of Table 2. The critical mechanism gives the lowest value of the bearing capacity pressure among the mechanisms

considered, is listed in parentheses in column 8. The ratios of calculated to measured strengths in column 10 of Table 2 show that the upper bound solutions predict the test results remarkably well for the case $e/b = 0$, and reasonably well for $e/b = 1/3$. The ratios range from 0.98 to 1.03 for $e/b = 0$ and 1.07 to 1.30 for $e/b = 1/3$. For the large ratio of $e/b = 2/3$, the upper bound solutions may over-estimate the bearing capacity by as much as 86 percent. This difference may be explained by the fact that local plastic flow of concrete for the case of large ratios of e/b is considerably less than that of small ratios of e/b , because hydrostatic pressure (or lateral confinement of the material due to the hoop stresses) around the punch cannot be induced high enough to permit the application of limit analysis.

6.2 Hawkins' Test Results [11]

The test results reported in Ref. 11 and those calculated from the present upper bound solutions are compared in Table 3 for specimens with $h/2a \leq 8$ and $b/a \leq 4$. The direct tensile strength of the concrete used in the theoretical calculations is estimated to be $f'_c/12$. The ratios of calculated to measured strengths listed in column 8 show that the upper bound limit analysis for a square punch on a square block predicts the results reasonably well. Although all the tests correspond to the extreme eccentricity ratio $e/b = 1 - a/b$, yet the calculated to measured strengths are in error only for the range from 1.19 to 1.53. Moreover, it is reported in Ref. 5 that the load carrying capacity for a double punch specimen (Fig. 1) is higher than that of a similar specimen which is supported directly on the steel bed

of a testing machine, as was the case in Hawkins' tests. This would suggest that a better correlation between the theoretical predictions of upper bound limit analysis and the results of double punch tests may be expected.

6.3 Approximate Solutions

The bearing capacity of a block with an eccentric punch load (Fig. 1b) may be estimated directly from the solution of the axially loaded situation (Fig. 1a) by assuming that the rigid punch load acts only across an effective block width $2b'$, and this width forms a concentric block with the punch. Thus, for example, for the case of a circular punch on a circular cylinder, this effective cylinder width may be taken to be $b' = b - e$ as shown by the dashed circle in Fig. 12. The material outside the radius b' is assumed to have no effect on the bearing capacity of the cylinder. These approximate solutions are summarized in columns 9 and 11 of Table 2. The observed bearing capacity is seen to be in good agreement with the approximate theoretical estimates.

7. CONCLUSIONS

The solutions presented here are a continuation of an investigation reported in Ref. 2. The problem considered here is closely related to the bearing strength of the anchorage zone of a prestressed concrete beam. More important, these solutions provide additional theoretical and experimental evidence as to the validity and limitations of the theory of perfect plasticity as applied to bearing capacity

problems in concrete. In the analysis, it was found that the upper bound theorem of limit analysis may be used to predict the bearing strength of an eccentrically loaded concrete block. However, when the eccentricity ratio of the punch load is large, crack propagation does enter for such a situation. An appropriate fracture mechanics for concrete is needed. Nevertheless, the solutions obtained herein still provide a reasonable upper bound for fractured concrete.

8. ACKNOWLEDGEMENTS

The research reported here was supported by the National Science Foundation under Grant GK-14274 to Lehigh University.

9. NOTATION

a	half-length of the side of the square punch or the radius of punch
b	half-length of the side of the square block or the radius of the circular cylinder
c	half-length of the side of the square cable duct or the radius of the circular cable duct
C	cohesion
D_A	ratio of energy dissipation per unit area, Eq.(1)
f'_c	concrete cylinder strength
f'_t	direct tensile strength
h	block or cylinder height
\bar{q}^u	bearing pressure over the total punch area

q^u	bearing pressure over the net bearing area
α, β, γ	angular parameters which define various mechanisms
$\Delta, \Delta_D, \Delta_R$	velocity variable of a mechanism
δw	discontinuous velocity across a failure plane
$\delta u, \delta v$	discontinuous tangential and normal velocity of δw
ϕ	friction angle of concrete
θ	angle between the velocity vector δw and its component δu , Fig. 2

REFERENCES

1. Sundara Raja Iyengar, K. T. and Yogananda, C. V.
A THREE-DIMENSIONAL STRESS DISTRIBUTION PROBLEM IN THE ANCHORAGE ZONE OF A POST-TENSIONED CONCRETE BEAM, Magazine of Concrete Research, Vol. 18, No. 55, pp. 75-84, June 1966.
2. Chen, W. F. and Drucker, D. C.
BEARING CAPACITY OF CONCRETE BLOCKS OR ROCK, Journal of the Engineering Mechanics Division, American Society of Civil Engineers, Vol. 95, No. EM4, Proc. Paper 6742, pp. 955-978, August 1969.
3. Drucker, D. C., Greenberg, H. J., and Prager, W.
EXTENDED LIMIT DESIGN THEOREMS FOR CONTINUOUS MEDIA, Quarterly Applied Mathematics, Vol. 9, pp. 381-389, 1952.
4. Chen, W. F.
EXTENSIBILITY OF CONCRETE AND THEOREMS OF LIMIT ANALYSIS, Journal of the Engineering Mechanics Division, American Society of Civil Engineers, Vol. 96, No. EM3, Proc. Paper 7369, pp. 341-352, June 1970.
5. Hyland, M. W. and Chen, W. F.
BEARING CAPACITY OF CONCRETE BLOCKS, Journal of the American Concrete Institute, Vol. 67, pp. 228-236, March 1970.
6. Chen, W. F.
DOUBLE PUNCH TEST FOR TENSILE STRENGTH OF CONCRETE, Journal of the American Concrete Institute, Vol. 67, pp. 993-995, December 1970.

7. Carson, J. L. and Chen, W. F.
STRESS-STRAIN RELATIONS FOR RANDOM WIRE REINFORCED CONCRETE,
Fritz Engineering Laboratory Report No. 370.1, Lehigh Uni-
versity, Bethlehem, Pennsylvania, October 1970.
8. Carson, J. L. and Chen, W. F.
BEARING CAPACITY OF RANDOM WIRE REINFORCED CONCRETE BLOCKS,
Fritz Engineering Laboratory Report No. 370.4, Lehigh Uni-
versity, Bethlehem, Pennsylvania, December 1970.
9. Drucker, D. C.
A MORE FUNDAMENTAL APPROACH TO STRESS-STRAIN RELATIONS, Pro-
ceedings, First U. S. National Congress for Applied Mechanics,
American Society of Mechanical Engineers, pp. 487-491, 1951.
10. Chen, W. F.
PLASTIC INDENTATION OF METAL BLOCKS BY FLAT PUNCH, Journal
of the Engineering Mechanics Division, American Society of
Civil Engineers, Vol. 96, No. EM3, Proc. Paper 7370, pp. 353-
363, June 1970.
11. Hawkins, N. M.
THE BEARING STRENGTH OF CONCRETE LOADED THROUGH RIGID PLATES,
Magazine of Concrete Research, Vol. 20, No. 62, pp. 31-40,
March 1968.

TABLE 1 - MECHANISM 2

Bearing Capacity of Circular and Square Long Blocks
with a Concentric Cable Duct $\varphi = 20^\circ$

$\frac{f'_c}{f'_t}$	$\frac{b}{a}$	$\frac{c}{a}$	Angle in Degrees			$\frac{q_u}{f'_c}$	Min. $\frac{h}{2a}$
			α	β	γ		
10	2	0	22.7	57.3	-12.7	2.9	3.6
		0.6	16.0	57.3	-12.7	1.5	4.8
	4	0	14.7	57.3	-12.7	7.4	6.4
		0.6	9.0	57.3	-12.7	5.9	8.8
14	2	0	22.8	49.6	-20.4	2.6	4.0
		0.6	15.4	49.6	-20.4	1.4	5.4
	4	0	13.9	49.6	-20.4	6.9	7.4
		0.6	8.1	49.6	-20.3	5.6	10.4

TABLE 2

Bearing Capacity of Circular Punch on Circular Blocks -
Double Punch Test*

(1) Test No.	(2) f'_c ksi	(3) f'_t ksi	(4) $\frac{f'_c}{f'_t}$	(5) $\frac{h}{2a}$	(6) $\frac{e}{b}$	(7)	(8)		(9)	(10)	(11)					
						q/f'_c					Tests	Theory ⁺	Mech.	Approx. ⁺	$\frac{(8)}{(7)}$	$\frac{(9)}{(7)}$
1	6.37	0.56	11.4	2.66	0	2.53	2.49	(3)	2.49	0.98	0.98					
2					2.23	2.38	(3)	2.18	1.07	0.98						
3					1.75	2.18	(3)	1.58	1.25	0.90						
4	6.45	0.57	11.3	4.00	0	3.10	3.19	(3)	3.19	1.03	1.03					
5					2.53	3.09	(3)	2.70	1.22	1.07						
6					1.85	2.85	(3)	1.79	1.54	0.97						
7	6.39	0.55	11.5	5.33	0	3.74	3.82	(3)	3.82	1.02	1.02					
8					2.93	3.70	(3)	3.08	1.26	1.05						
9					1.93	3.31	(7)	2.06	1.79	1.06						
10	6.32	0.54	11.7	6.66	0	4.35	4.40	(3)	4.40	1.01	1.01					
11					3.29	4.27	(3)	3.51	1.30	1.07						
12					2.13	3.31	(7)	2.30	1.86	0.87						

* $b/a = 4$ for all specimens

⁺ $f'_c = 12 f'_t$, $\varphi = 20^\circ$

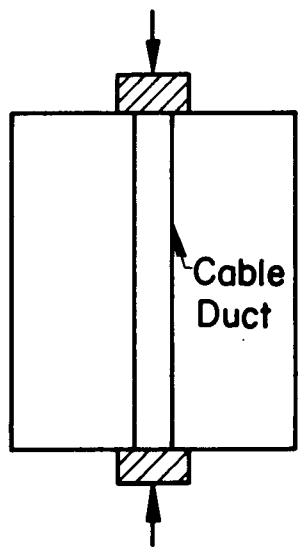
TABLE 3

Bearing Capacity of Square Punches on Square Blocks -
Hawkins' Tests* [11]

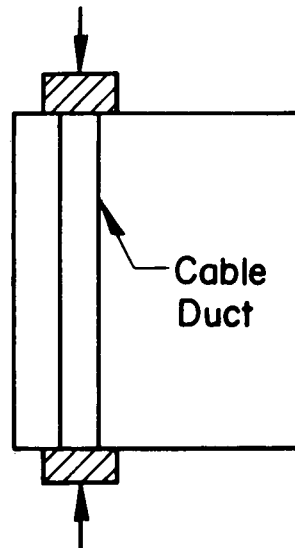
(1) Test No.	(2) 2a (in.)	(3) $\frac{b}{a}$	(4) $\frac{h}{2a}$	(5) $\frac{e}{b}$	(6)		(7)		(8) $\frac{(7)}{(6)}$
					q/f' _c				
					Tests	Theory ⁺	Mech.		
1	1.72	3.50	7.00	0.714	1.99	2.98	(6)	1.50	
2	2.42	2.48	4.96	0.597	1.75	2.08	(6)	1.19	
3	3.00	2.00	4.00	0.500	1.40	1.91	(4)	1.36	
4	1.72	3.50	7.00	0.714	1.95	2.98	(6)	1.53	
5	2.00	3.00	6.00	0.667	1.77	2.45	(6)	1.38	
6	3.00	2.00	4.00	0.500	1.52	1.91	(4)	1.26	
7	2.00	3.00	6.00	0.667	1.91	2.45	(6)	1.28	
8	3.00	2.00	4.00	0.500	1.71	1.91	(4)	1.12	
9	2.00	3.00	6.00	0.667	1.68	2.45	(6)	1.46	
10	3.00	2.00	4.00	0.500	1.38	1.91	(4)	1.39	

*All specimens are 6 inch cubes

⁺f'_c = 12 f'_t, φ = 20°



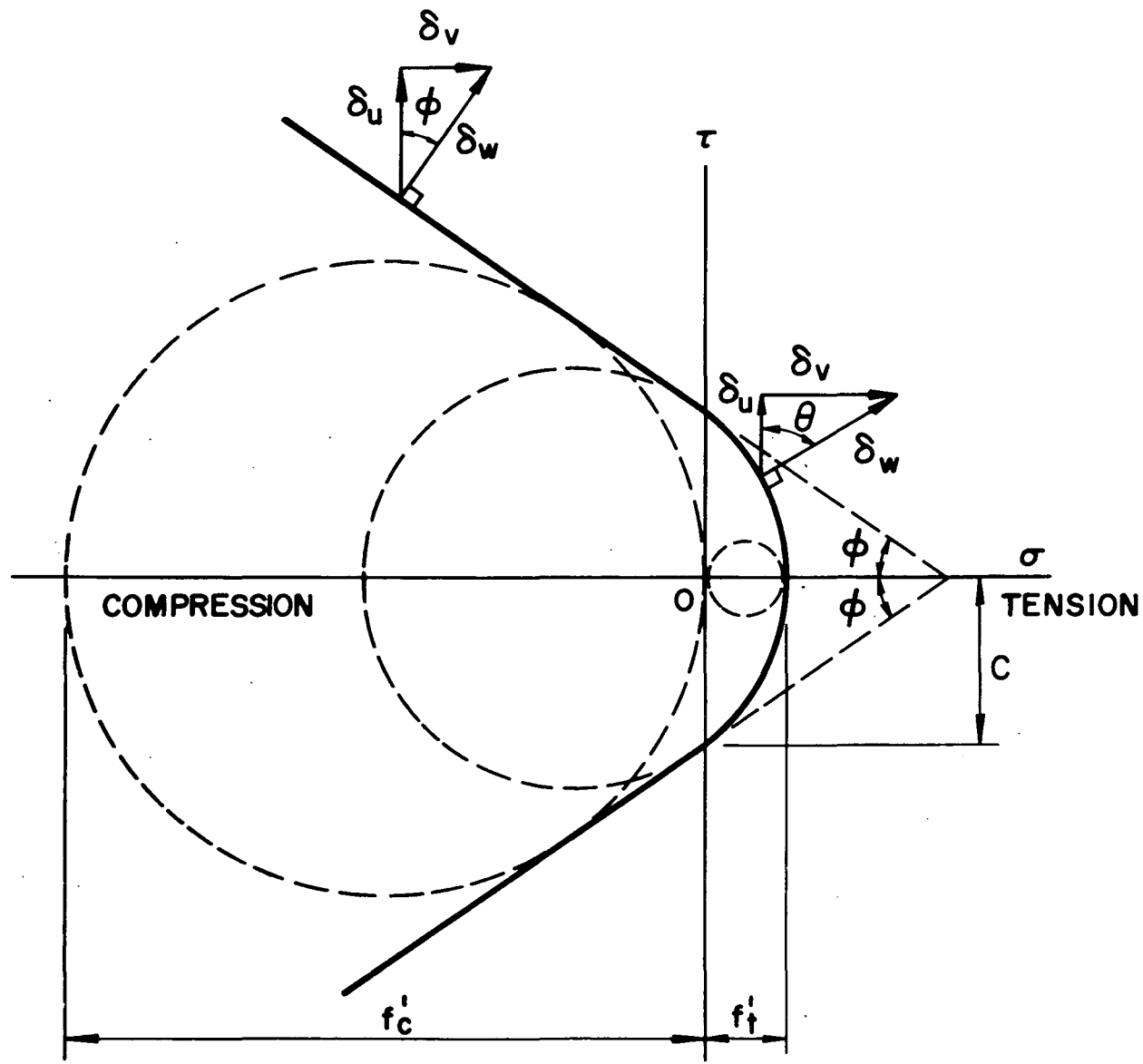
(a) Concentric Duct



(b) Eccentric Duct

Fig. 1 Simplified Problem of the End Bearing
in a Post-Tensioned Concrete Beam

Fig. 2 Modified Mohr-Coulomb Yield Criterion



MECHANISM I

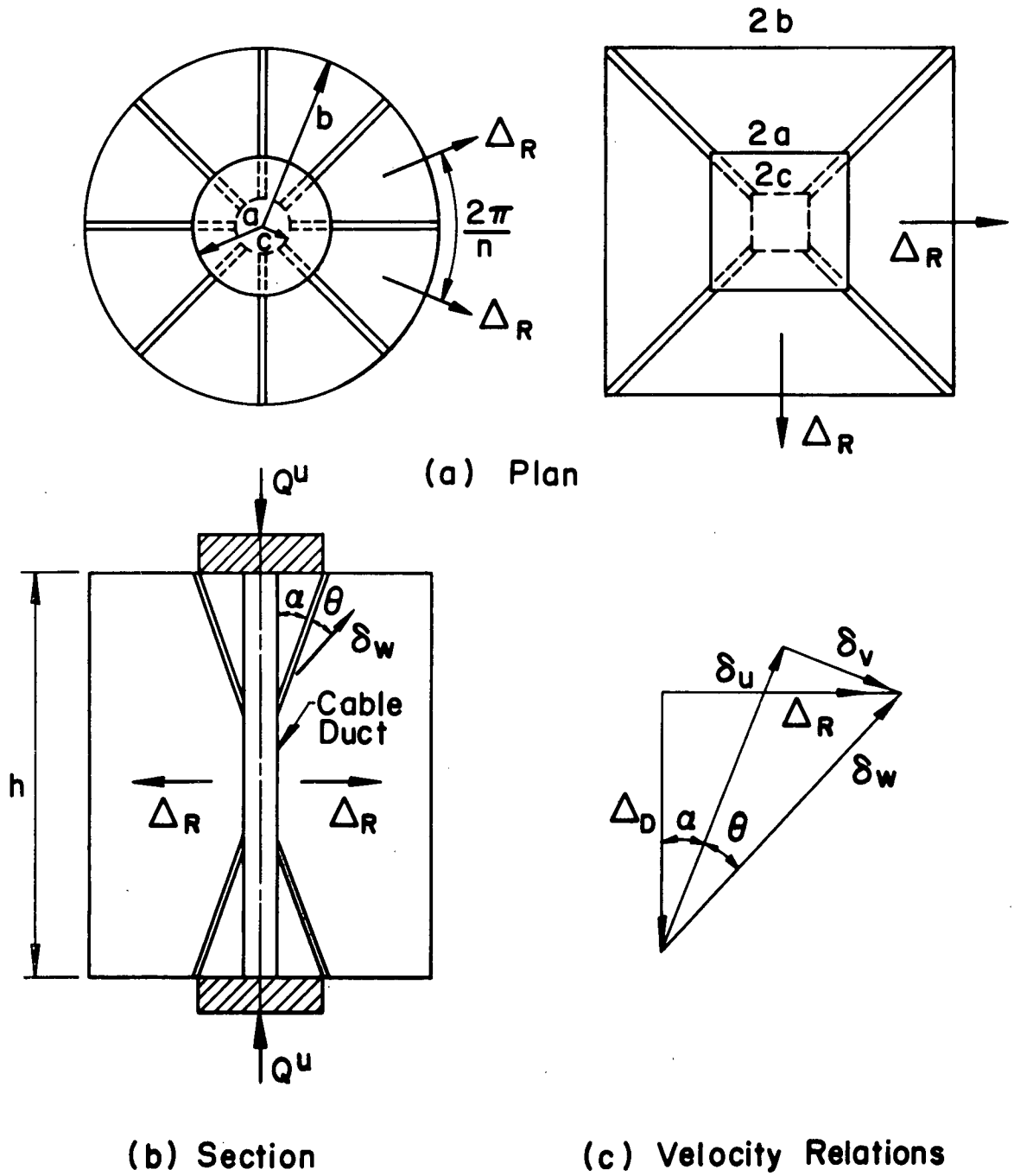


Fig. 3 Short Circular and Square Blocks with a Concentric Cable Duct

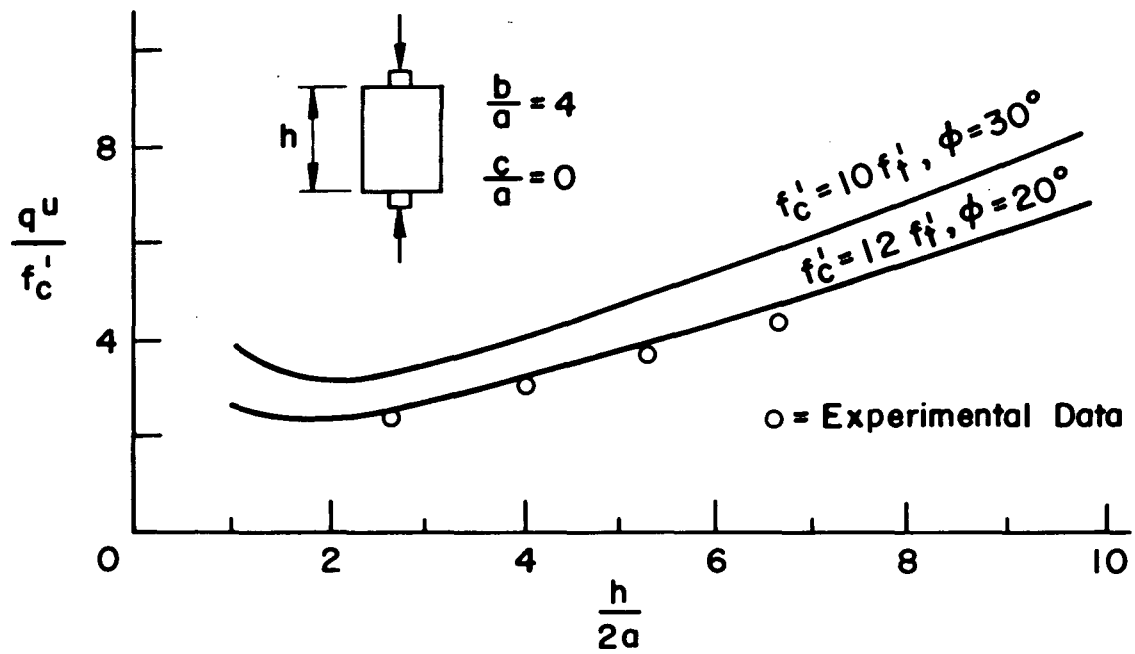


Fig. 4 Comparison of Upper Bounds with Test Data for Two Circular Punches on a Short Circular Block

MECHANISM 2

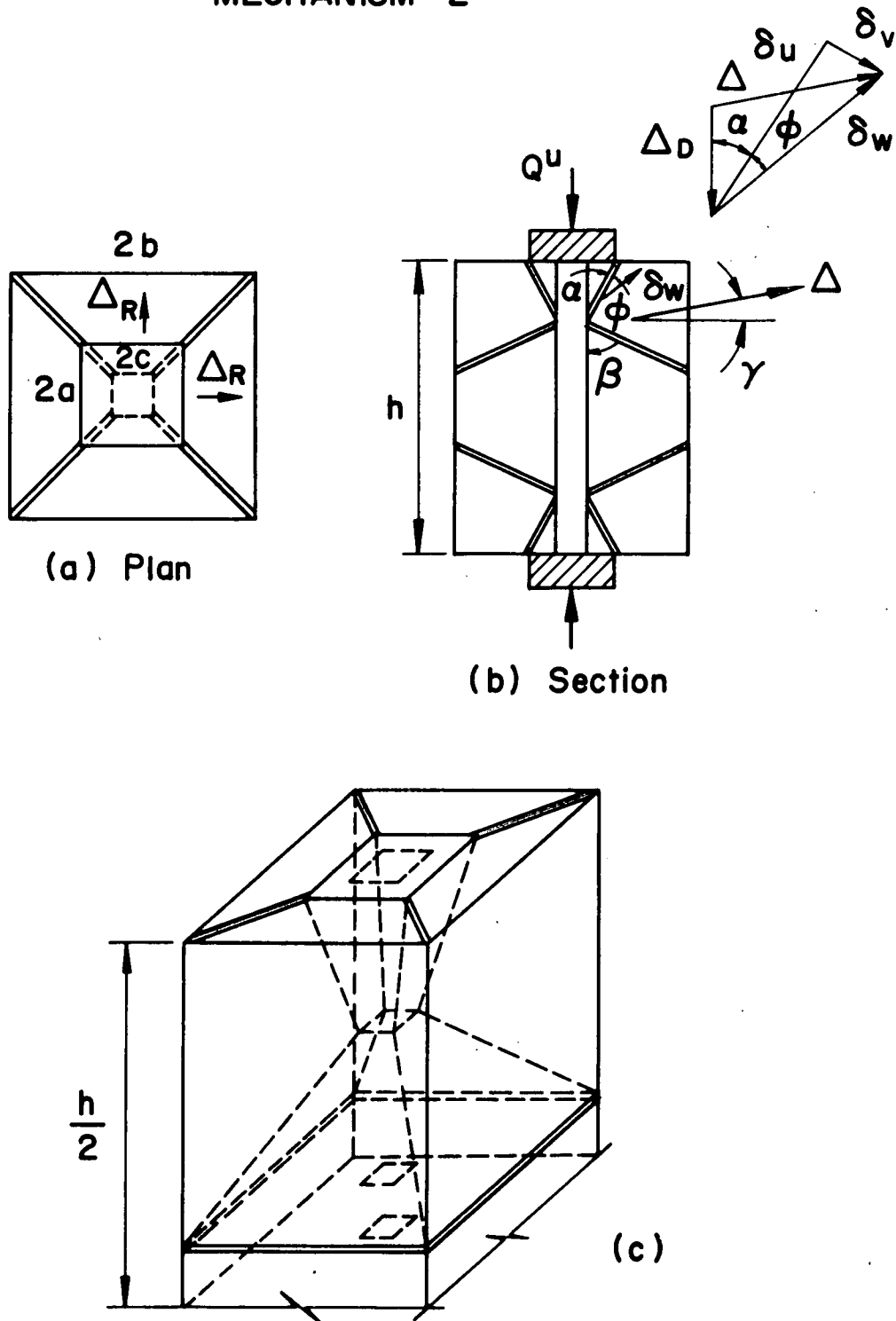


Fig. 5 Long Circular and Square Blocks with a Concentric Cable Duct

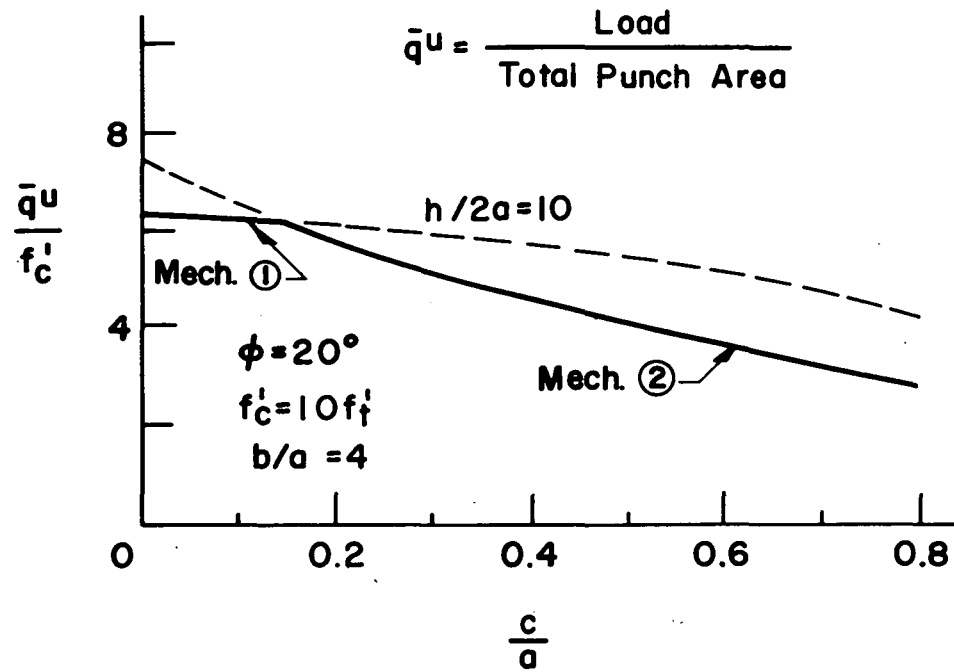
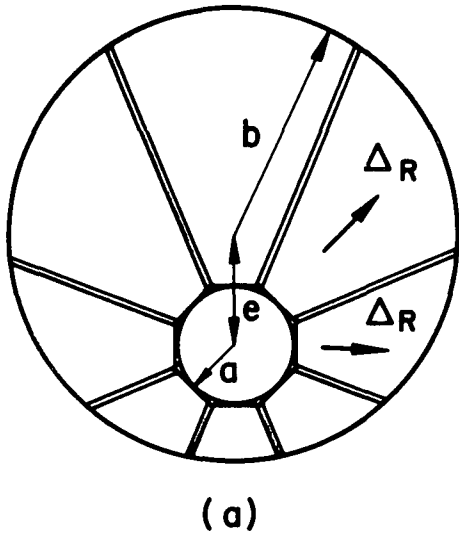


Fig. 6 Concrete Blocks with a Concentric Cable Duct

MECHANISM 3



MECHANISM 4

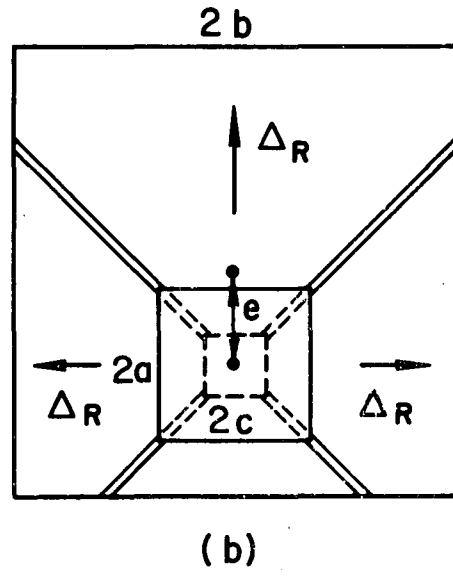


Fig. 7 Short Concrete Blocks with an Eccentric Cable Duct - Small Eccentricity

MECHANISM 2'

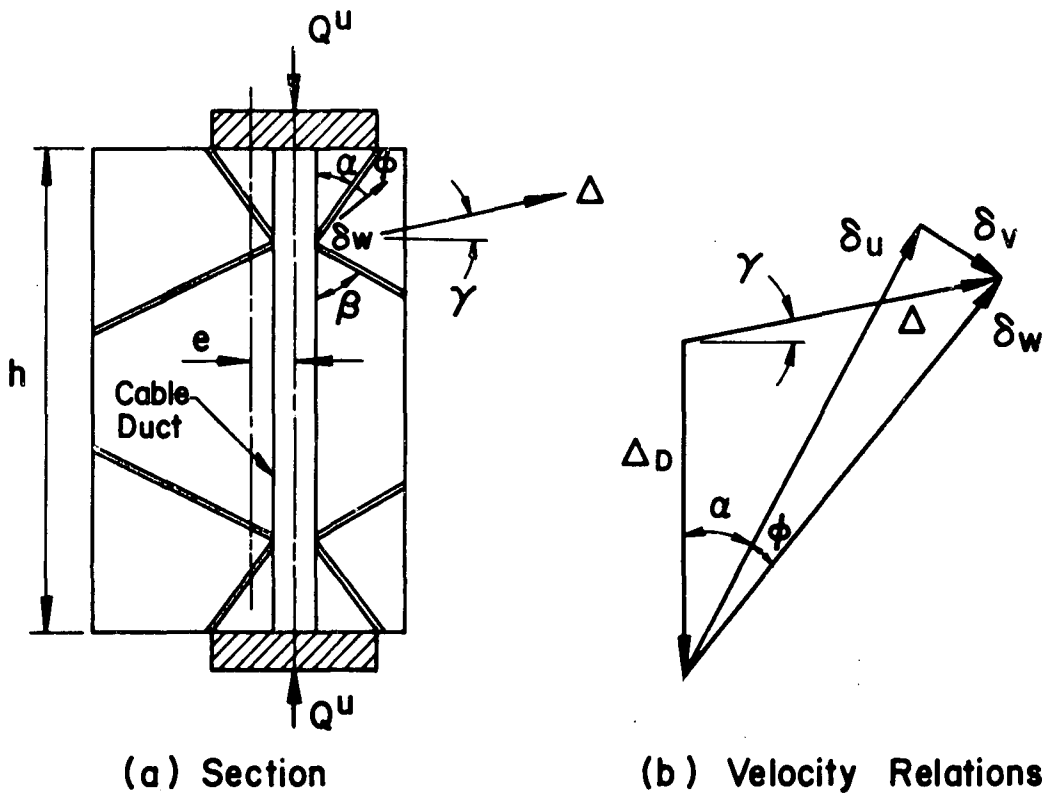
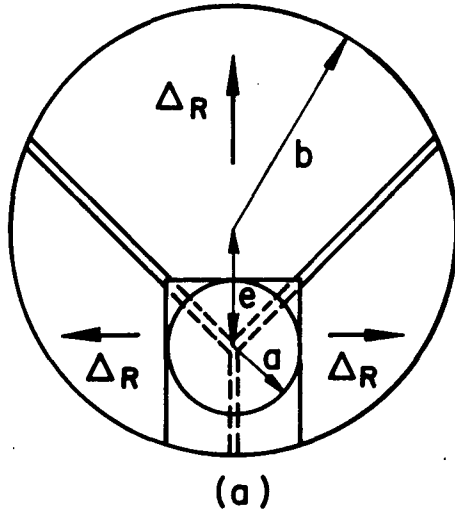


Fig. 8 Long Concrete Blocks with an Eccentric Cable Duct - Small Eccentricity

MECHANISM 5



MECHANISM 6

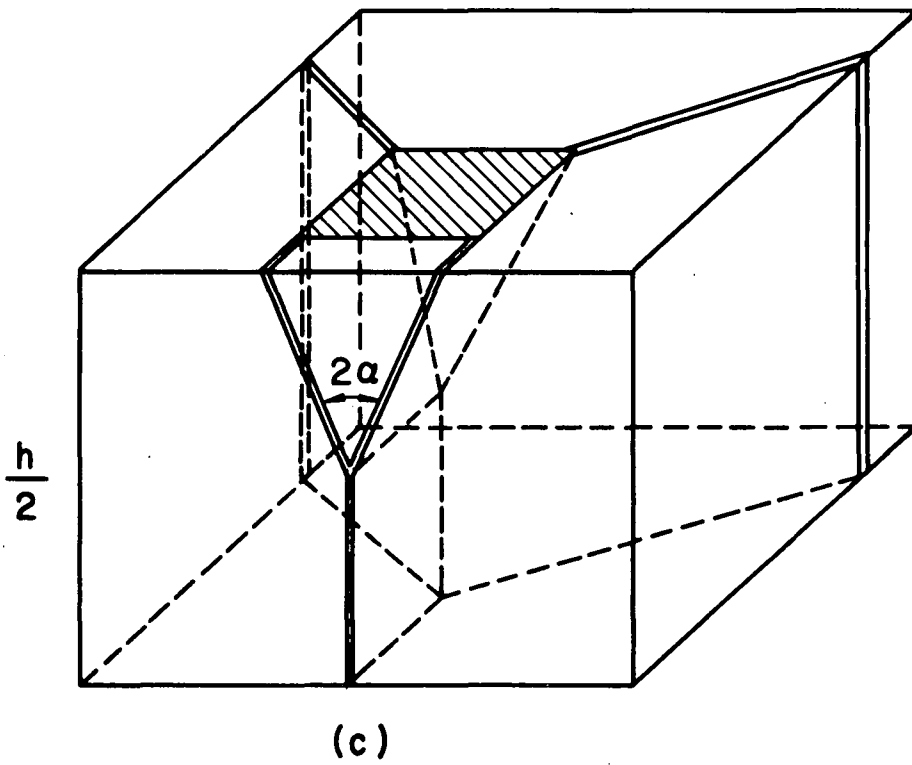
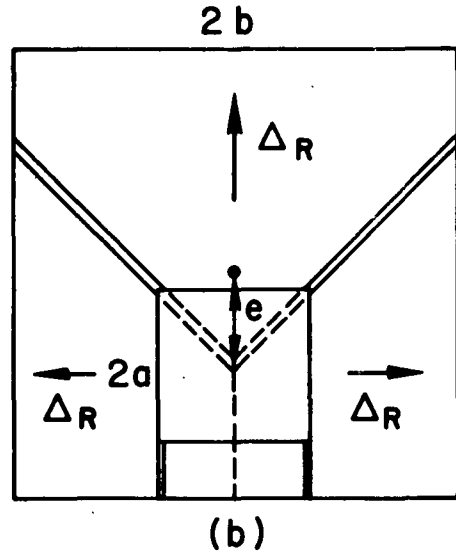
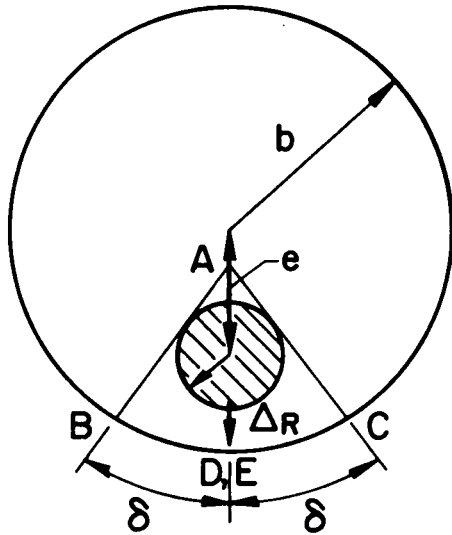


Fig. 9 Short Concrete Blocks with an Eccentric Cable Duct - Large Eccentricity

MECHANISM 7



MECHANISM 8

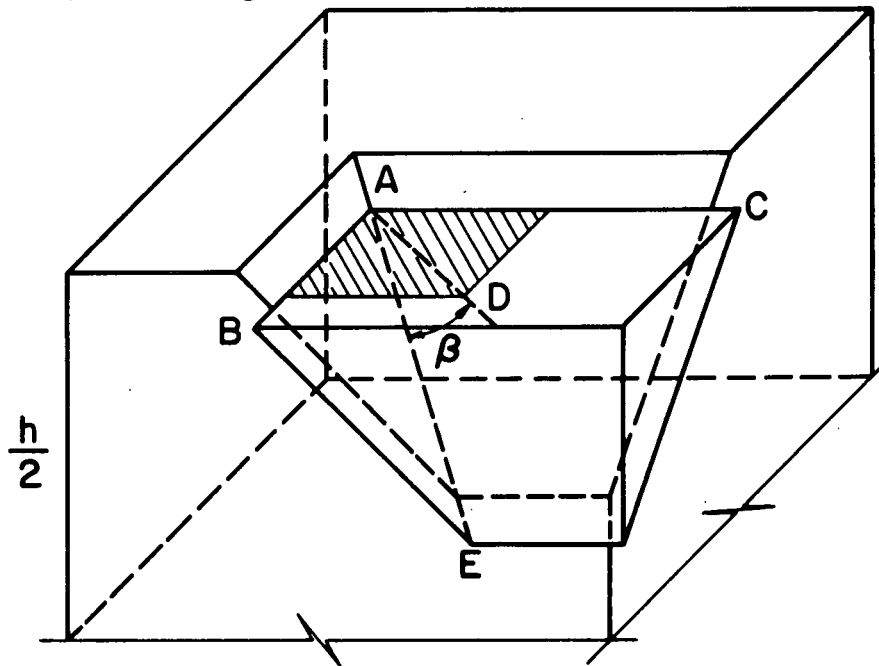
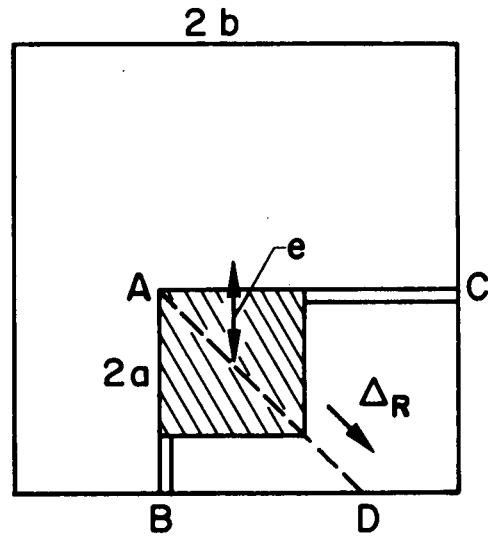


Fig. 10 Long Concrete Blocks with an Eccentric Cable Duct - Large Eccentricity

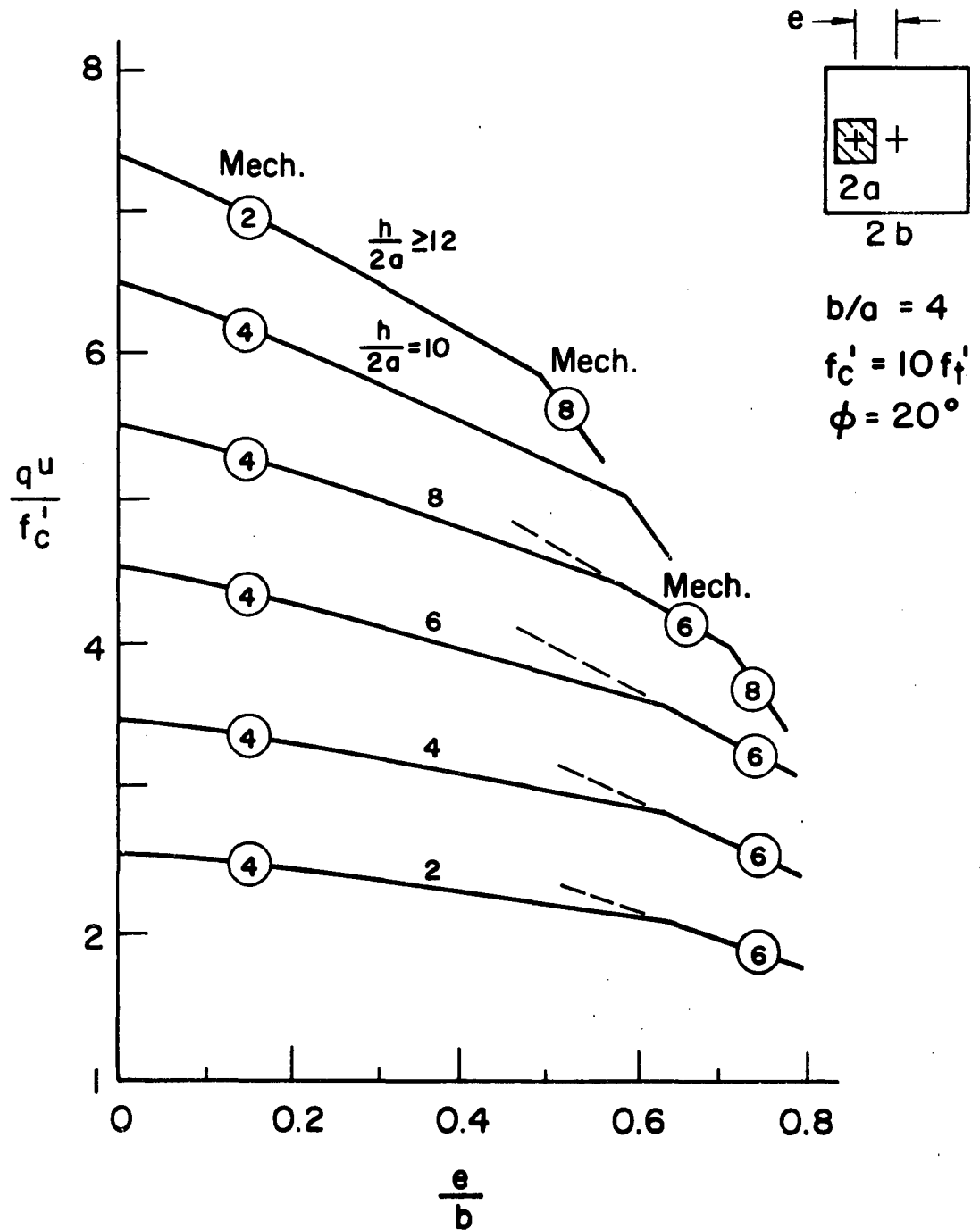


Fig. 11 Bearing Capacity of an Eccentrically Loaded Square Block

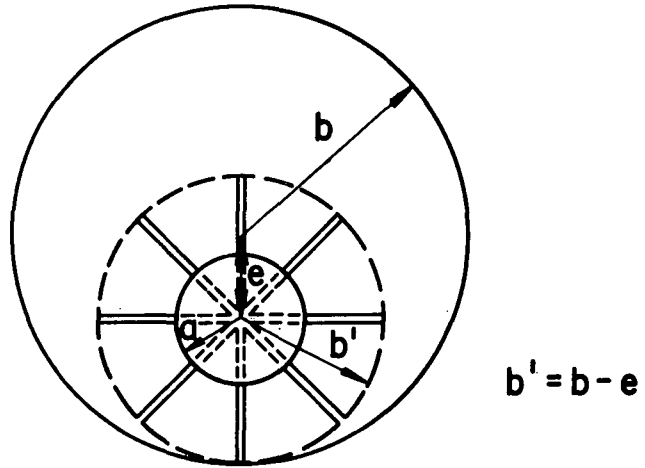


Fig. 12 Approximate Solution to an Eccentrically Loaded Block